J Therm Anal Calorim (2012) 107:1083–1091
DOI 10.1007/s10973-011-1848-3

Thermal degradation of differently substituted Cyclopentyl Polyhedral Oligomeric Silsesquioxane (CP-POSS) nanoparticles

I. Blanco · L. Abate · F. A. Bottino · P. Bottino · M. A. Chiacchio

Received: 25 March 2011 / Accepted: 3 August 2011 / Published online: 23 August 2011

Abstract Seven variously substituted derivatives of polyhedral oligomeric silsesquioxanes (POSSs) with general formula $R_7R'_1$ $(SiO_{1.5})_8$, where R- and R′- were a cyclopentyl and a substituted phenyl group, respectively, were prepared in this study, and their compositions were checked by elemental analysis, ^1H NMR and ^{13}C NMR spectroscopy. The compounds obtained were studied by TG and DTA techniques, in both flowing nitrogen and static air atmospheres, to draw useful information about their resistance to thermal degradation. Experiments, performed in the 35–700 °C temperature range, showed different behaviours between the two used atmospheres. The formation of volatile compounds only, with a near-complete mass loss, was observed under nitrogen; by contrast, in oxidative environment, a solid residue ($\approx$50% in every case) was obtained because of the formation of SiO_2 as indicated by the FTIR spectra performed. The results obtained for the various compounds investigated were discussed and compared with each other, and heat resistance classifications in the studied environments were made.

Keywords POSS · Silsesquioxanes · Thermogravimetric analysis · Thermal degradation

I. Blanco (✉) · F. A. Bottino
Department of Industrial and Mechanical Engineering, University of Catania, V.le A. Doria, 6, 95125 Catania, Italy
e-mail: iblanco@dmfci.unict.it

L. Abate
Department of Physical and Chemical Methodologies for Engineering, University of Catania, V.le A. Doria, 6, 95125 Catania, Italy

P. Bottino
Department of Pharmaceutical Sciences, University of Catania, V.le A. Doria 6, 95125 Catania, Italy

M. A. Chiacchio
Department of Chemical Sciences, University of Catania, V.le A. Doria, 6, 95125 Catania, Italy

Introduction

In recent years, polymer–nanoparticle composite materials have attracted the interest of a number of researchers because of their synergistic and hybrid properties derived from several components [1–8].

An approach adopted to develop better materials is to create inorganic–organic composite materials in which inorganic building blocks are incorporated into organic polymers.

The use of nanoparticles as polymer additives, when compared with the traditional ones, is more advantageous because lower loading is required [9–13].

Microsized particles used as reinforcing agents scatter light, thus reducing optical transmittance and clarity. By contrast, efficient nanoparticles dispersion, combined with good polymer–particle interfacial adhesion, eliminates scattering and allows for the exciting possibility of developing strong yet transparent films, coatings and membranes [9–11].

Polyhedral oligomeric silsesquioxanes (POSSs) are a type of hybrid inorganic/organic material of the formula $(RSiO_{1.5})n$, or R*n*T*n*, where organic substituents are attached to a silicon–oxygen cage.

POSS nanostructured chemicals can be incorporated into common plastics via copolymerization [9, 14–17], grafting [9, 10] or blending [9–11], thereby offering a special opportunity for the preparation of new thermoset

[18–21] and thermoplastic materials [10, 11, 16, 17, 22–24].

The incorporation of POSS derivatives into polymeric materials can lead to substantial improvements in polymer properties including increases in service temperature [25], oxidation resistance [10], surface hardening [10] and mechanical properties [26] as well as reductions in flammability [27], heat evolution [28] and viscosity [29] during processing. These improvements have been shown in a wide range of thermoplastic and thermoset systems, e.g. methacrylates [22], styrenes [23], norbornenes [30], ethylenes [31], epoxies [18], etc.

The different behaviour of each specific POSS in various resins is attributable to size of POSS cage, nature of organic periphery, concentration and solubility of POSS in the resin. These factors determine whether POSS is incorporated as isolated and uniformly dispersed molecules or as phase-separated particles. The ability of POSS to be dispersed at molecular level is the key to realize enhancement of their physical properties. In order to be able to modulate the properties of POSS-reinforced polymers, the thermal properties of POSS nanoparticles together with their solubility and compatibility with the polymer matrix must be investigated.

A typical POSS nanoparticle is characterized by an inorganic Si_8O_{12} nanostructured skeleton surrounded by eight organic groups, such as alkyl, aryl, or any of their derivatives, linked to silicon atoms by covalent bond [32, 33].

The most common molecular formula of POSS is $(RSiO_{1.5})_8$ or $R_7R'_1$ $(SiO_{1.5})_8$ where R and R′ are organic substituents.

The nature of these side groups, which can be either unreactive or chemically reactive, determines the solubility in conventional solvents, the compatibility with host polymer matrices, and then the capability to undergo nanometric dispersion, and the physical and mechanical properties of the resulting hybrid nanocomposites.

The size of these molecules lies in a range of 1–3 nm. A POSS molecule with an isobutyl periphery has a diameter of approximately 1.5 nm [34]. Then, POSSs are isodimensional spherical particles which can form well-dispersed nanocomposites and, for this reason, have been used as fillers in a number of polymeric matrices with the aim to improve polymer properties.

Since the POSS-based nanocomposites are materials of relevant and increasing technological importance because of their excellent properties, this author group has planned a wide research programme on the synthesis and the characterization of new thermally stable POSS nanocomposites having PS and polyolefins as polymer matrices. It is well known in the literature that the unreactive organic functionalities covalently bonded to silicon atoms are responsible for the compatibility of POSSs with various polymers as well as for their thermal behaviour [24, 35–37]. Also, it is known that aliphatic-bonded groups improve solubility and compatibility with polymer matrices but worsen thermal properties, whilst aromatic groups act in the opposite way [37]. In particular, the literature data concerning octamethyl-, octaisobutyl- and octaisooctyl POSSs in PP matrix have evidenced a better compatibility of octaisobutyl- than octamethyl- derivative, whilst no further improvement of compatibility was observed for the octaisooctyl- with respect to the octaisobutyl-compound, thus suggesting an improvement of compatibility as a function of the number of carbon atoms in the alkyl chain, at least within certain limits [38].

Since both high thermal stability and good compatibility with polymers are demanded for the POSSs used as nanofillers to obtain good performance nanocomposites, we have planned to synthesize and study, in a preliminary stage, new POSSs with the general formula $R_nR'_{(8-n)}(SiO_{1.5})_8$ (where R = alkyl group and R′ = aryl group), to investigate if, and if so how much, thermal stability and compatibility with polymers are affected by the R/R′ ratio and R′ nature, aiming to find a *n* value for which POSS exhibits maximum thermal stability together with good compatibility.

In this study, which is the starting point of the wider over-reported plan of research, we studied some hetero-substituted silsesquioxanes of general formula $R_7R'_1(SiO_{1.5})_8$, where R- and R′- were a cyclopentyl and a substituted phenyl group, respectively (Fig. 1). Cyclopentyl group, which has five carbon atoms in the aliphatic ring, was selected because it would ensure a good compatibility with the selected polymeric matrices on the basis of results in Ref.

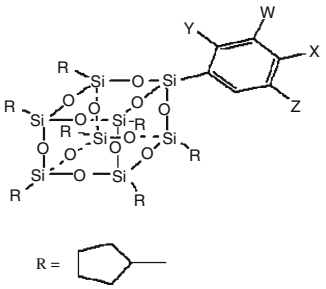

Fig. 1 Molecular structure of hetero-substituted POSS derivatives

Sample	Substituents			
1	X = H	Y = H	Z = H	W = H
2	X = CH_3	Y = H	Z = H	W = H
3	X = OCH_3	Y = H	Z = H	W = H
4	X = F	Y = H	Z = H	W = H
5	X = H	Y = H	Z = CH_3	W = CH_3
6	X = F	Y = F	Z = H	W = H
7	X = F	Y = F	Z = F	W = H

[38]. Also, on the basis of the few articles reported in the literature, POSSs with seven cyclopentyl groups would have sufficiently high thermal stability [13]. The aim of this study was to assess how the thermal stability in both inert and oxidative atmospheres changed with the nature of the substituents in the aromatic ring. The synthesized silsesquioxanes were characterized by elemental analysis, ^{1}H NMR and ^{13}C NMR spectroscopy, and the thermal stability was assessed by the determination of the temperature at 5% mass loss ($T_{5\%}$).

Experimental

Materials

Phenyltrichlorosilane and *p*-tolyltrichlorosilane have been purchased from Aldrich Co. and used as received. 4-Fluorophenyltrichlorosilane, 2,4-difluorophenyltrichlorosilane, 2,4,5-trifluorophenyltrichlorosilane, 3,5-dimethylphenyltrichlorosilane and 4-methoxyphenyltrichlorosilane were prepared from the appropriate Grignard reagent and $SiCl_4$ [39, 40]. The cyclopentyltrisilanol (c $C_5H_9)_7$–Si_7O_9 $(OH)_3$ was prepared according to the literature methods [41, 42]. Tetrahydrofuran was distilled over a Na-benzophenone mixture.

Compounds **1**–**7** were prepared by corner capping reaction of cyclopentyltrisilanol with the suitable aryltrichlorosilane. The same procedure was used for all compounds. The synthesis of **2** is given as an example.

A solution of cyclopentyltrisilanol (2.18 g, 2.5 mmol) and triethylamine (0.79 g, 7.82 mmol) in 40 mL of dry THF was cooled in an ice bath and a solution of *p*-tolyltrichlorosilane (0.61 g, 2.7 mmol) in 40 mL of dry THF was added dropwise under stirring. After the addition was completed, the mixture was allowed to warm to room temperature and stirred overnight. The suspension was filtered, and the $Et_3N{\cdot}HCl$ precipitate was washed with THF (2 × 20 mL). The combined organic filtrate was reduced under vacuum, and the resulting slurry was dissolved in a minimum amount of THF and poured into stirred methanol (5 folds). After filtration and drying under reduced pressure, the white solid obtained was crystallized from CH_2Cl_2/MeCN mixture to give 2.08 g of the required compound (84% yield).

Yield, ^{1}H NMR, ^{13}C NMR spectroscopy and elemental analysis

^{1}H NMR and ^{13}C NMR spectra were recorded on a Varian Unity Inova instrument (^{1}H 500 MHz) in $CDCl_3$ as solvent. Chemical shifts are in ppm (δ) from TMS as internal standard.

The ^{1}H NMR and ^{13}C NMR data found for the various compounds investigated were the following:

Compound **1**

Yield 91.2%. ^{1}H NMR: 7.66 (dd, 2H), 7.41 (dd, 1H), 7.35 (dd, 2H), 1.75 (m, 14H), 1.54 (m, 42 H), 1.01 (m, 7H). ^{13}C NMR: 134.03, 132.19, 130.16, 127,59 (aromatic), 27.32, 27.02, 26.96 (CH_2), 22.25(CH). Anal. Calcd for $C_{41}H_{68}Si_8O_{12}$: C 50.40, H 7.02. Found: C 49.95, H 7.10.

Compound **2**

Yield 84.1%. ^{1}H NMR: 7.55 (d, 2H), 7.18 (d, 2H), 2.36 (s, 3H), 1.74 (m, 14H), 1.56 (m, 42 H), 1.02 (m, 7H). ^{13}C NMR: 140.08, 134.09, 128.66, 128.41 (aromatic), 27.32, 27.03, 26.97 (CH_2), 22.28 (CH), 21.61 (CH_3). Anal. Calcd for $C_{42}H_{70}Si_8O_{12}$: C 50.90, H 7.12. Found: C 50.61, H 7.14.

Compound **3**

Yield 77.9%. ^{1}H NMR: 7.59 (d, 2H), 6.90 (d, 2H), 3.82 (s, 3H), 1.75 (m, 14H), 1.52 (m, 42 H), 1.01 (m, 7H). ^{13}C NMR: 161.23, 135.64, 123.40, 112.73 (aromatic), 55.01 (OCH_3), 27.34, 27.02, 26.97 (CH_2), 22.27 (CH). Anal. Calcd for $C_{42}H_{70}Si_8O_{13}$: C 50.10, H 7.01. Found: C 50.20, H 7.09.

Compound **4**

Yield 81.2%. ^{1}H NMR: 7.64 (dd, 2H), 7.05 (dd, 2H), 1.75 (m, 14H), 1.53 (m, 42 H), 1.01 (m, 7H). ^{13}C NMR: 164,38, 136.15, 127.92, 114.86 (aromatic), 27.31, 27.01, 26.95 (CH_2), 22.27 (CH). Anal. Calcd for $C_{41}H_{67}FSi_8O_{12}$: C 49.49, H 6.79. Found: C 49.02, H 6.83.

Compound **5**

Yield 72.3%. ^{1}H NMR: 7.28 (s, 2H), 7.06 (s, 1H), 2.31(s, 6H), 1.76 (m, 14H), 1.53 (m, 42 H), 1.01 (m, 7H). ^{13}C NMR: 136.87, 131.00, 130.00, 114.86 (aromatic), 27.31, 27.01, 26.95 (CH_2), 22.27 (CH), 21.32 (CH_3). Anal. Calcd for $C_{43}H_{72}Si_8O_{12}$: C 51.39, H 7.22. Found: C 51.03, H 7.31.

Compound **6**

Yield 66.0%. ^{1}H NMR: 7.55 (dd, 1H), 6.86 (dd, 1H), 6.74 (dd, 1H), 1.75 (m, 14H), 1.52 (m, 42 H), 1.03 (m, 7H). ^{13}C NMR: 167.69, 165.17, 137.44, 114.60, 111.00, 103.40 (aromatic), 27.25, 27.05 (CH_2), 22.23 (CH). Anal. Calcd

for $C_{41}H_{66}F_2Si_8O_{12}$: C 48.61, H 6.52. Found: C 48.73, H 6.57.

Compound **7**

Yield 60.4%. ^{1}H NMR: 7.35 (m, 1H), 6.87 (m, 1H), 1.75 (m, 14H), 1.54 (m, 42 H), 1.02 (m, 7H). ^{13}C NMR: 166.22, 164.18, 147.24, 114.64, 110.93, 103.31 (aromatic), 27.28, 27.01, 26.97 (CH_2), 22.28 (CH). Anal. Calcd for $C_{41}H_{65}F_3Si_8O_{12}$: C 47.76, H 6.36. Found: C 47.44, H 6.40.

IR spectroscopy

The Fourier Transform Infrared (FTIR) absorption spectra were recorded by a Perkin Elmer model Spectrum 100 spectrometer, using a universal ATR sampling accessory.

Thermal analysis

A Shimadzu DTG-60 simultaneous DTA-TG apparatus was used for both thermogravimetric analysis (TG) and differential thermal analysis (DTA). The calibrations of temperature, heat flow and weight were performed following the procedure reported in the instruction manual of equipment [43] using as standard materials: indium (NIST SRM 2232), tin (NIST SRM 2220) and zinc (NIST SRM 2221a) for temperature; indium (NIST SRM 2232) for heat flow and a set of exactly weighed samples supplied by Shimadzu for weight. All the calibrations of equipment were repeated every 2 weeks.

Scannings were carried out in the temperature range 35 to 700 °C, at the heating rate of 10 °C min^{-1}, under flowing nitrogen (0.02 L min^{-1}) and in a static air atmosphere. Samples of about 5×10^{-3} g, placed in a 40-μL platinum open pan, were used for experiments. For TG, the sample weight as a function of temperature was monitored and recorded by a PC connected with the DTG-60 apparatus. At the end of each run, the experimental data were utilized to plot the percentage of undegraded sample W/Wo% as a function of temperature, where W_o and W were the weights of sample at the starting point and during scanning. For DTA analysis, the heat flow of sample was monitored and recorded by the PC connected with the DTG-60 apparatus, to evaluate enthalpy and temperature of the observed phase transitions.

Results and discussion

The thermal behaviour of our compounds was studied by TG and DTA experiments in the temperature range 35–700 °C, in both flowing nitrogen and static air atmosphere.

The thermogravimetric curves evidenced different behaviours in the studied environments.

The TG and DTG curves in inert atmosphere (Figs. 2, 3) showed for all the studied compounds a first degradation stage, in every case included in the 300–450 °C temperature range, associated with the most part of mass loss (83.3–90.6%), immediately followed by a another lesser one at higher temperature. Low quantities of residue were found at 700 °C for compounds **1**, **3**, **4** and **7** only (Table 1).

By contrast, the TG and DTG curves in oxidative atmosphere (Figs. 4, 5) evidenced more complex degradation processes for all compounds, with an overall mass loss, after the complete temperature scan, ranging from 44.4 to 51.3%.

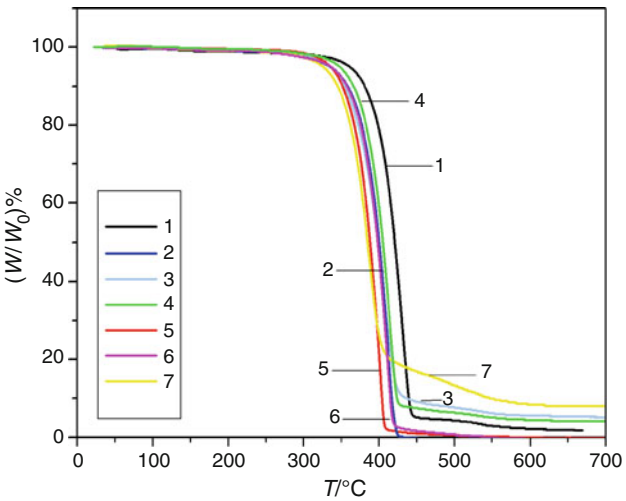

Fig. 2 TG curves under nitrogen flow of differently substituted Polyhedral Oligomeric Silsesquioxanes (POSSs)

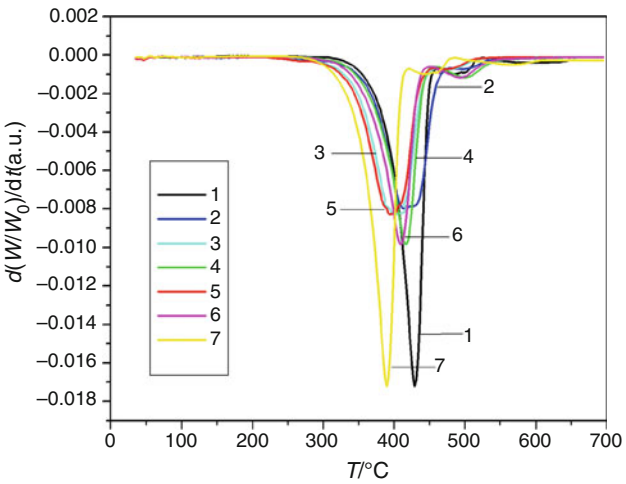

Fig. 3 DTG curves under nitrogen flow of differently substituted Polyhedral Oligomeric Silsesquioxanes (POSSs)

Table 1 Temperatures at 5% mass loss ($T_{5\%}$), temperatures at maximum rate of weight loss (T_m) for the main degradation stage and residue % at 700 °C of the studied silsesquioxanes in flowing nitrogen and in static air atmosphere

	Nitrogen flow			Air static atmosphere		
Compound	$T_{5\%}$ °C	T_m °C	Residue %	$T_{5\%}$ °C	T_m °C	Residue %
1	361.2	431.7	1.7	307.8	331.1	52.4
2	335.2	412.5	0	278.0	301.4	49.3
3	336.2	406.9	5.1	295.8	318.8	51.9
4	347.6	414.6	4.2	303.8	324.4	55.6
5	335.4	403.2	0	287.4	304.2	53.2
6	336.1	411.4	0	293.6	322.0	49.5
7	325.7	390.1	8.0	297.9	334.9	48.7

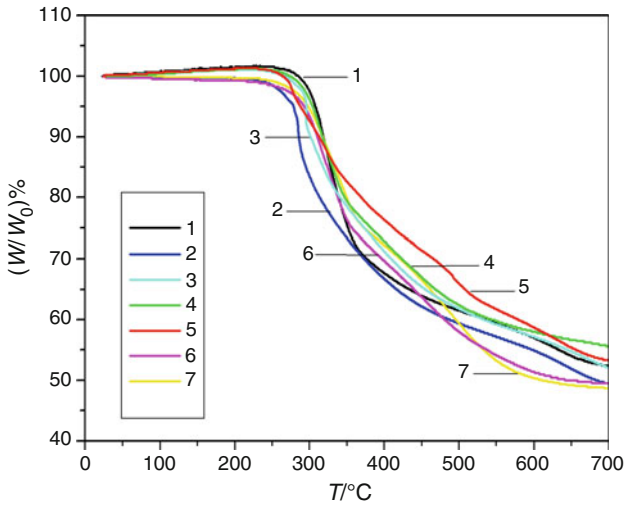

Fig. 4 TG curves in static air atmosphere of differently substituted Polyhedral Oligomeric Silsesquioxanes (POSSs)

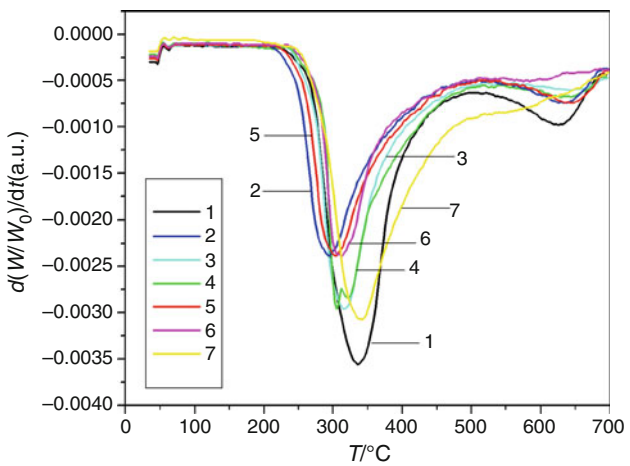

Fig. 5 DTG curves in static air atmosphere of differently substituted Polyhedral Oligomeric Silsesquioxanes (POSSs)

The initial temperatures of decomposition (T_i), which are a measure of thermal stability, can be obtained by the TG curves as the intersection between the starting mass line and the maximum gradient tangent to the TG curve. Since for our compounds it was difficult to single out reliable T_i values in air owing to the increment of weight observed for some samples in oxidative atmosphere, probably because of oxidation and crosslinking of material [35], the temperatures at 5% mass loss ($T_{5\%}$) were determined and used for the comparisons amongst the various compounds investigated.

The temperatures of DTG peaks (T_m), which are the temperatures at maximum weight loss rate, as well as the $T_{5\%}$ values, were much lower in air than under nitrogen (Table 1).

The DTA analyses confirmed the different behaviours of our compounds in the experimental atmospheres used. A broad endothermic DTA peak, followed, in some cases, by another little and irregular endothermic one at higher temperature, was obtained, for all investigated compounds, under nitrogen (Fig. 6). It is important to note that a very little thermal effect, starting at about 100 °C in every case, was observed at temperatures lower than DTA peaks. By contrast, in static air atmosphere, all studied silsesquioxanes exhibited an irregular exothermic DTA peak, followed by one or more other exothermic ones at higher temperatures, as shown in Fig. 7. The temperatures of the main DTA peak (T_p) of various compounds are reported in Table 2.

The overall picture of the results from thermal experiments suggests some considerations:

– the TG curves and the related quantitative data of weight loss indicate that the degradation mechanism under nitrogen of the studied silsesquioxanes is

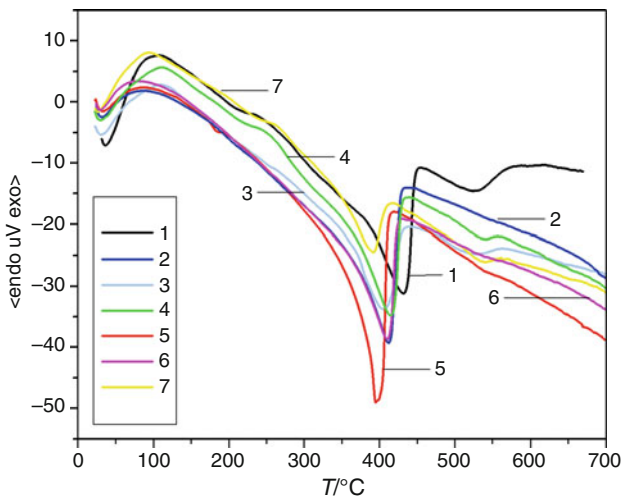

Fig. 6 DTA curves under nitrogen flow of differently substituted Polyhedral Oligomeric Silsesquioxanes (POSSs)

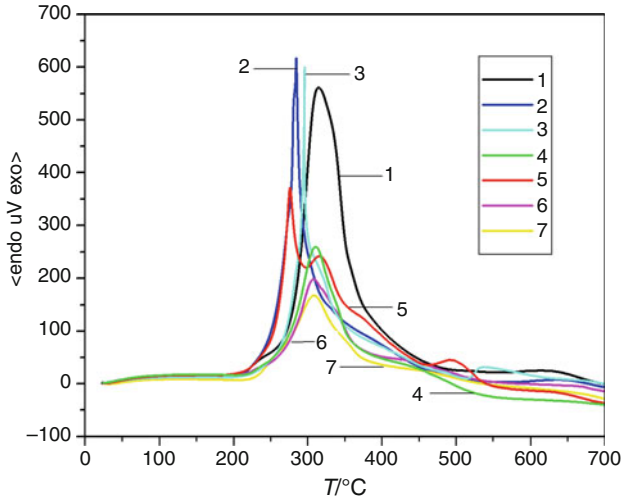

Fig. 7 DTA curves in static air atmosphere of differently substituted Polyhedral Oligomeric Silsesquioxanes (POSSs)

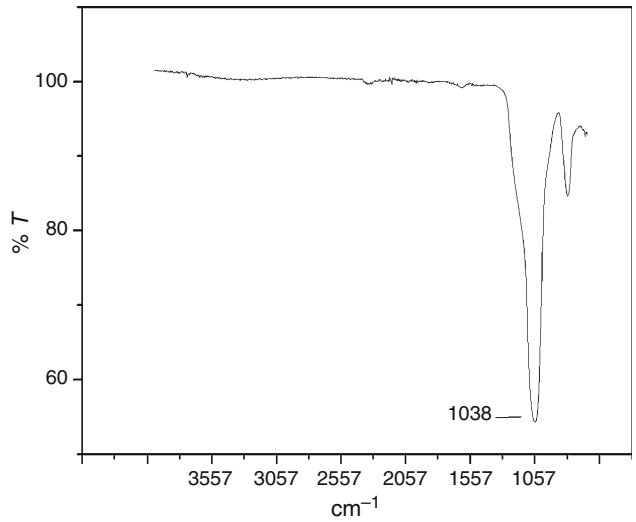

Fig. 8 FTIR spectrum of the residue of compound **7** after thermal degradation under nitrogen flow

Table 2 Temperature (T_p) and enthalpy ($-\Delta H$) of DTA peak of the studied silsesquioxanes in flowing nitrogen and in static air atmosphere

Compound	Nitrogen flow		Air static atmosphere	
	T_p/°C	$(-\Delta H)$/kJ g^{-1}	T_p/°C	$(-\Delta H)$/kJ g^{-1}
1	431.9	−2.41	314.4	33.98
2	412.7	−3.04	284.4	38.57
3	405.1	−1.72	285.4	35.24
4	414.7	−2.10	310.2	30.57
5	394.9	−2.18	276.0	40.72
6	410.1	−2.68	307.9	26.99
7	391.7	−1.19	308.2	17.71

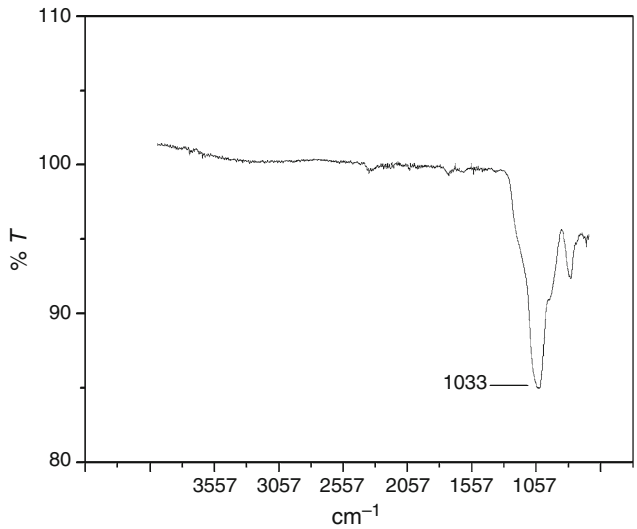

Fig. 9 FTIR spectrum of the residue of compound **7** after thermal degradation in static air atmosphere

different from that in air, where oxygen appears to play an active role in the decomposition process. The little quantities of solid residue obtained from the degradations in flowing nitrogen after the complete temperature scan (35 ÷ 700 °C) are formed essentially by SiO_2, as evidenced by the performed FTIR spectra. In Fig. 8, the FTIR spectrum of the residue from compound **7** is reported as an example.

Also, the solid residue obtained from the oxidative degradations up to 700 °C appears because of the formation of SiO_2, as supported by stoichiometric calculations on the mass loss. This finding is in agreement with the literature data on similar compounds [37] and was also confirmed by the FTIR spectra of the formed solid residues. In Fig. 9, the spectrum of the residue obtained in static air atmosphere from compound **7** is reported as an example;

– the initial decomposition temperatures of our compounds in both the studied environments, which are correlated with the $T_{5\%}$ values here determined, are of the same magnitude [44] or, in some cases, higher than similar compounds [37, 45], thus indicating a good thermal stability.

For all the investigated silsesquioxanes, the degradation in air started at lower temperature than in flowing nitrogen. In particular, for each compound, the difference of $T_{5\%}$ values between nitrogen and air fell in the 28 ÷ 53 °C range, whilst higher differences (100 ÷ 135 °C) were found for the T_m values in the two used atmosphere;

– the $T_{5\%}$ values found in inert environment do not allow us to make a heat resistance classification amongst the various compounds because four of them (compounds **2**, **3**, **5** and **6**) were substantially the same. The unsubstituted silsesquioxane (Compound **1**) appears the most thermally stable in nitrogen.

The 2,4,5-trifluoro derivative (Compound **7**) in inert atmosphere shows lower initial decomposition temperature than all the other compounds investigated. Since the decomposition of a sample can be observed by TG only when the produced gases can freely effuse from the sample (and then when the partial pressure of the evolved gaseous products exceeds the ambient pressure), the lower $T_{5\%}$ value found for compound **7** could be due to lower packing density of crystals, and then to easier effusion of decomposition products.

The results of the degradation experiments in oxidative environment were rather quite different than those under nitrogen because, even though the differences of $T_{5\%}$ values amongst various compounds in static air atmosphere were not very large, they allowed us to make a heat resistance classification. On the basis of this classification, the unsubstituted silsesquioxane (Compound **1**) appears, also in oxidative experimental conditions, the most thermally stable, followed by the F-substituted derivatives. It is interesting to note that the $T_{5\%}$ value of **7** in oxidative environment is similar to those of other fluorinated compounds. The different behaviour of **7** in the two experimental conditions investigated could be due to the different mechanism of degradation in static air atmosphere in respect of flowing nitrogen. The methyl derivatives (Compounds **2** and **5**) appear, on the basis of the $T_{5\%}$ values found, the lesser thermally stable compounds amongst those here studied, followed by the methoxy-derivative (Compound **3**).

– the introduction of various substituents (methyl, methoxy- and F-) into the phenyl group lowers the thermal stability, as evidenced by the lower $T_{5\%}$ values of the substituted phenyl derivatives (compounds **2**–**7**) in respect of the unsubstituted compound **1**. Nevertheless, in our opinion, for the evaluation of the overall thermal stability of a compound, we must take into account not only the heat resistance (which depends on the initial decomposition temperature, and then on the $T_{5\%}$), but also the degradation rate. This last parameter is more relevant when the initial decomposition temperatures of the compounds compared are close with each other. This is the case of the compounds investigated in this study. From the data in Table 1, we observe that the differences amongst the $T_{5\%}$ value of the unsubstituted compound **1** and those of compounds **6** and **7** are not high, resulting in only 14.2 °C and 9.9 °C, respectively. By contrast, the differences ($T_m - T_{5\%}$), which can be roughly considered a measure of the degradation rate, are 23.3 °C for compound **1**, and 28.4 °C and 37.0 °C for the compounds **6** and **7**, respectively, thus indicating lower degradation rates for the F-derivatives. These results suggest that the introduction of more than one halogen atom into the phenyl group produces oxidation inhibition.
– the temperatures of endothermic DTA peaks under nitrogen (Table 2) were substantially the same as those of corresponding DTG peaks (Table 1), thus, suggesting that the endothermic effects measured are due to the decomposition process of silsesquioxanes investigated. It is important to note that the DTA curves show a very little deviation from baseline starting from 100 °C, whilst the corresponding DTG peaks start at much higher temperatures. In order to interpret the very little and not evaluable thermal effect at temperatures lower than decomposition process, we verified by an equipment for melting point determination (room temperature–400 °C) if our compounds showed, before decomposition, solid–liquid transitions. The performed experiments excluded melting processes, but showed the formation of white sublimate in every case. The thermal effects from about 100 °C up to the initial decomposition temperatures could be thus attributed, in our opinion, to sublimation processes of some impurities, such as residual solvent and/or other small compounds remaining after synthesis [46].

An analogous correspondence amongst the temperatures of exothermic DTA peaks and DTG peaks was found in static air atmosphere. The DTA curves of all the studied compounds start, also in this case, from about 100 °C and show higher irregularity than under nitrogen because of complex oxidative processes occurring in air, which overlap to sublimation process. The enthalpy values associated with DTA peaks are reported in Table 2 also.

The exothermic enthalpy values associated with the principal DTA peak of various compounds in static air atmosphere (Table 2) are in agreement with the oxidative nature of the degradation processes, and decrease according to the following order: **5** > **2** > **3** > **1** > **4** > **6** > **7**. These results appear to be in agreement with the level of oxidizability of the variously substituted phenyl groups, as suggested by the enthalpy of combustion values of benzene, toluene, m-xylene, anisole, F-benzene and 1,3-difluorobenzene from the literature (http://webbook.nist.gov/chemistry/fluid/), which decrease in the same order than the corresponding POSSs here studied.

The endothermic ΔH values associated with the degradations in flowing nitrogen support the non-oxidative nature of the decomposition processes in inert environment.

Conclusions

This study is the first part of a wider research concerning the synthesis of new variously substituted POSSs having high thermal stability and good compatibility and solubility in polymer matrices. In this article, some cyclopentyl POSSs mono-substituted by a phenyl group bearing various substituents were synthesized by a simple route, were characterized and their degradation was followed by both TG and DTA techniques. The results have been encouraging because all compounds showed high thermal stability, thus suggesting the possibility of their use also in quite drastic conditions.

Acknowledgements Financial support was provided by the Ministry of Education, University and Research (MIUR) in the frame of an Italian research program (COFIN 2007).

References

1. Zaitsev VS, Filimonov DS, Presnyakov IA, Gambino RJ, Chu B. Physical and chemical properties of magnetite and magnetite-polymer nanoparticles and their colloidal dispersions. J Colloid Interf Sci. 1999;212:49–57.
2. Haraguchi K, Farnworth R, Ohbayashi A, Takehisa T. Compositional effects on mechanical properties of nanocomposite hydrogels composed of poly (N,N-dimethylacrylamide) and clay. Macromolecules. 2003;36:5732–41.
3. Hu Y, Chen JF, Zhang HT, Li TW, Xue X. Using silicon dioxide nanosphere gaps to confine growth of single-crystal nickel sulfide nanowires in polyacrylamide gel. Scripta Mater. 2006;55:131–4.
4. Yu SL, Zuo XT, Bao RL, Xu X, Wang J, Xu J. Effect of SiO_2 nanoparticle addition on the characteristics of a new organic-inorganic hybrid membrane. Polymer. 2009;50:553–9.
5. Chrissafis K, Paraskevopoulos KM, Tsiaoussis I, Bikiaris D. Comparative study of the effect of different nanoparticles on the mechanical properties, permeability, and thermal degradation mechanism of HDPE. J Appl Polym Sci. 2009;112:1606–18.
6. Avella M, Cosco S, Di Lorenzo ML, Di Pace E, Errico ME. Influence of $CaCO_3$ nanoparticles shape on thermal and crystallization behavior of isotactic polypropylene based nanocomposites. J Therm Anal Calorim. 2005;80(1):131–6.
7. Ramezanzadeh B, Attar MM, Farzam M. Effect of ZnO nanoparticles on the thermal and mechanical properties of epoxy-based nanocomposite. J Therm Anal Calorim. 2011;103(2):731–9.
8. Viratyaporn W, Lehman RL. Effect of nanoparticles on the thermal stability of PMMA nanocomposites prepared by in situ bulk polymerization. J Therm Anal Calorim. 2011;103(1):267–73.
9. Lichtenhan JD, Schwab JJ. Bridging the centuries with SAMPE's materials and processes technology. In: Loud S, editor. 45th international SAMPE symposium and exhibition. Society for the advancement of material and process engineering (SAMPE), Covina, CA. vol. 45, p. 185–191, 2000.
10. Phillips SH, Blanski RL, Svejda SA, Haddad TS, Lee A, Lichtenhan JD, Feher FJ, Mather PT, Hsiao BS. New insight into the structure-property relationships of hybrid (inorganic/organic) POSS^{tm} thermoplastics. Mater Res Soc Symp Proc. 2000;628: CC4.6.1–10.
11. Blanski RL, Phillips SH, Chaffee K, Lichtenhan JD, Lee A, Geng HP. The synthesis of hybrid materials by the blending of polyhedral oligosilsesquioxanes into organic polymers. Polym Prepr. 2000;41:585–6.
12. Fina A, Monticelli O, Camino G. POSS-based hybrids by melt/reactive blending. J Mater Chem. 2010;20:9297–305.
13. Cordes DB, Lickiss PD, Rataboul F. Recent developments in the chemistry of cubic polyhedral oligosilsesquioxanes. Chem Rev. 2010;110:2081–173.
14. Voronkov MG, Vavrent'yev VI. Polyhedral oligosilsesquioxanes and their homo derivatives. Top Curr Chem. 1982;102:199–236.
15. Mather PT, Jeon HG, Haddad TS. Strain recovery in POSS hybrid thermoplastics. Polym Prepr. 2000;41(1):528–9.
16. Haddad TS, Choe E, Lichtenhan JD. Hybrid styryl-based Polyhedral Oligomeric Silsesquioxane (POSS) polymers. Mater Res Soc Symp Proc. 1996;435:25–32.
17. Haddad TS, Stapleton R, Jeon HG, Mather PT, Lichtenhan JD, Phillips SH. Nanostructured hybrid organic/inorganic materials: silsesquioxane modified plastics. Polym Prepr. 1999;40(1):496–7.
18. Lee A, Lichtenhan JD. Viscoelastic responses of polyhedral oligosilsesquioxane reinforced epoxy systems. Macromolecules. 1998;31(15):4970–4.
19. dell Erba IE, Williams RJJ. Epoxy networks modified by multifunctional polyhedral oligomeric silsesquioxanes (POSS) containing amine groups. J Therm Anal Calorim. 2008;93(1):95–100.
20. Villanueva M, Martín-Iglesias JL, Rodríguez-Añón JA. Proupín-Castiñeiras J. Thermal study of an epoxy system DGEBA (n = 0)/mXDA modified with POSS. J Therm Anal Calorim. 2009;96(2):575–82.
21. Wang XT, Yang YK, Yang ZF, Zhou XP, Liao YG, Lv CC, Chang FC, Xie XL. Thermal properties and liquid crystallinity of side-chain azobenzene copolymer containing pendant polyhedral oligomeric silsequioxanes. J Therm Anal Calorim. 2010;102(2): 739–44.
22. Lichtenhan JD, Otonari YA, Carr MJ. Linear hybrid polymer building blocks: methacrylate-functionalized polyhedral oligomeric silsesquioxane monomers and polymers. Macromolecules. 1995;28(24):8435–7.
23. Haddad TS, Lichtenhan JD. Hybrid organic–inorganic thermoplastics: styryl-based polyhedral oligomeric silsesquioxane polymers. Macromolecules. 1996;29(22):7302–4.
24. Mantz RA, Jones PF, Chaffee KP, Lichtenhan JD, Ismail MK, Burmeister M. Thermolysis of Polyhedral Oligomeric Silsesquioxane (POSS) macromers and POSS–Siloxane copolymers. Chem Mater. 1996;8(6):1250–9.
25. Xu HY, Kuo SW, Lee JY, Chang FC. Glass transition temperatures of poly(hydroxystyrene-*co*-vinylpyrrolidone-*co*-isobutylstyryl polyhedral oligosilsesquioxanes). Polymer. 2002;43(19): 5117–24.
26. Pellice SA, Fasce DP, Williams RJJ. Properties of epoxy networks derived from the reaction of diglycidyl ether of bisphenol A with polyhedral oligomeric silsesquioxanes bearing OH-functionalized organic substituents. J Polym Sci Part B: Polym Phys. 2003;41(13):1451–61.
27. Philips SH, Gonzalez RI, ,Chaffee KP, Haddad TS, Hoflund GB, Hsiao BS, Fu BX. Remarkable AO resistance of POSS inorganic/organic polymer. In Loud S, editor. Bridging the centuries with SAMPE's materials and processes technology. 45th International SAMPE Symposium and Exhibition. Society for the Advancement of Material and Process Engineering (SAMPE), Covina, CA. 2000;45:1921–31.
28. Huang JC, He CB, Xiao Y, Mya KY, Dai J, Siow YP. Polyimide/POSS nanocomposites: interfacial interaction, thermal properties and mechanical properties. Polymer. 2003;44(16):4491–9.
29. Fu BX, Namani M, Lee A. Influence of phenyl-trisilanol polyhedral silsesquioxane on properties of epoxy network glasses. Polymer. 2003;44(25):7739–47.

30. Bharadwaj RK, Berry RJ, Farmer BL. Molecular dynamics simulation study of norbornene—POSS polymers. Polymer. 2000;41(19):7209–21.
31. Tsuchida A, Bolln C, Sernetz FG, Frey H, Mulhaupt R. Ethene and propene copolymers containing silsesquioxane side groups. Macromolecules. 1997;30(10):2818–24.
32. Harrison PG. Silicate cages: precursors to new materials. J Organomet Chem. 1997;542(2):141–83.
33. Baney RH, Itoh M, Sakakibara A, Suzuki T. Silsesquioxanes. Chem Rev. 1995;95(5):1409–30.
34. De Armitt C, Wheeler P. POSS keeps high temperature plastics flowing. Plast Addit Compd. 2008;10(4):36–9.
35. Bolln C, Tsuchida A, Frey H, Mulhaupt R. Thermal properties of the homologous series of 8-fold alkyl-substituted octasilsesquioxanes. Chem Mater. 1997;9(6):1475–9.
36. Fina A, Tabuani D, Frache A, Boccaleri E, Camino G. In: Le Bras M, Wilkie C, Bourbigot S, editors. Fire retardancy of polymers: new applications of mineral fillers. Cambridge, UK: Royal Society of Chemistry, 2005. p. 202–20
37. Fina A, Tabuani D, Carniato F, Frache A, Boccaleri E, Camino G. Polyhedral oligomeric silsesquioxanes (POSS) thermal degradation. Thermochim Acta. 2006;440(1):36–42.
38. Fina A, Tabuani D, Frache A, Camino G. Polypropylene–polyhedral oligomeric silsesquioxanes (POSS) nanocomposites. Polymer. 2005;46:7855–66.
39. Rosenberg SD, Walburn JJ, Ramsden HE. Preparation of some arylchlorosilanes with arylmagnesium chlorides. J Org Chem. 1957;22(12):1606–7.
40. Breed LW, Haggerty WJ Jr. Aryl and alkylchlorodialkoxysilanes. J Org Chem. 1960;25(1):126–8.
41. Feher FJ, Newman DA. Enhanced silylation reactivity of a model for silica surfaces. J Am Chem Soc. 1990;112(5):1931–6.
42. Feher FJ, Budzichowski TA, Blanski RL, Weller KJ, Ziller JW. Facile syntheses of new incompletely condensed polyhedral oligosilsesquioxanes: $[(c\text{-}C_5H_9)_7Si_7O_9(OH)_3]$, $[(c\text{-}C_7H_{13})_7Si_7O_9(OH)_3]$, and $[(c\text{-}C_7H_{13})_6Si_6O_7(OH)_4]$. Organometallics. 1991;10(7):2526–8.
43. Shimadzu DTG-60/60H Instruction manual. Shimadzu corporation. Kyoto, Japan: Analytical & Measuring Instruments Division; 2000.
44. Wu YC, Kuo SW. Synthesis and characterization of polyhedral oligomeric silsesquioxane (POSS) with multifunctional benzoxazine groups through click chemistry. Polymer. 2010;51(17):3948–55.
45. Hato MJ, Ray SS, Luyt AS. Thermal and rheological properties of POSS-containing poly(methyl methacrylate) nanocomposites. Adv Sci Lett. 2010;3(2):123–9.
46. Calzaferri G, Hoffmann R. The symmetrical octasilasesquioxanes $X_8Si_8O_{12}$: electronic structure and reactivity. J Chem Soc Dalton Trans. 1991;917–28.